Planar Thermal Hall Effect from Phonons in Cuprates

Lu Chen,[1,*] Léna Le Roux,[1] Gaël Grissonnanche,[1,2] Marie-Eve Boulanger,[1] Steven Thériault,[1] Ruixing Liang,[3,4] D. A. Bonn,[3,4] W. N. Hardy,[3,4] S. Pyon,[5,6] T. Takayama,[5,7] H. Takagi,[5,7,8,9] Ke-Jun Xu,[10,11,12] Zhi-Xun Shen,[10,11,12] and Louis Taillefer[1,4,†]

[1]*Institut quantique, Département de physique and RQMP, Université de Sherbrooke, Sherbrooke, Québec, Canada*
[2]*Laboratoire des Solides Irradiés, CEA/DRF/IRAMIS, CNRS, École Polytechnique, Institut Polytechnique de Paris, F-91128 Palaiseau, France*
[3]*Department of Physics and Astronomy, University of British Columbia, Vancouver, British Columbia, Canada*
[4]*Canadian Institute for Advanced Research, Toronto, Ontario, Canada*
[5]*Department of Advanced Materials Science, University of Tokyo, Kashiwa, Japan*
[6]*Department of Applied Physics, University of Tokyo, Tokyo, Japan*
[7]*Max Planck Institute for Solid State Research, Stuttgart, Germany*
[8]*Department of Physics, University of Tokyo, Tokyo, Japan*
[9]*Institute for Functional Matter and Quantum Technologies, University of Stuttgart, Stuttgart, Germany*
[10]*Geballe Laboratory for Advanced Materials, Stanford University, Stanford, California, USA*
[11]*Stanford Institute for Materials and Energy Sciences, SLAC National Accelerator Laboratory, Menlo Park, California 94025, USA*
[12]*Departments of Physics and Applied Physics, Stanford University, Stanford, California, USA*

(Received 20 October 2023; revised 22 April 2024; accepted 9 August 2024; published 11 October 2024)

A surprising "planar" thermal Hall effect, whereby the field is parallel to the current, has recently been observed in a few magnetic insulators; this effect has been attributed to exotic excitations such as Majorana fermions or chiral magnons. Here, we investigate the possibility of a planar thermal Hall effect in three different cuprate materials, in which the conventional thermal Hall conductivity κ_{xy} (with an out-of-plane field perpendicular to the current) is dominated by either electrons or phonons. Our measurements show that the planar κ_{xy} from electrons in cuprates is zero, as expected from the absence of a Lorentz force in the planar configuration. By contrast, we observe a sizable planar κ_{xy} in those samples where the thermal Hall response is due to phonons, even though it should, in principle, be forbidden by the high crystal symmetry. Our findings call for a careful reexamination of the mechanisms responsible for the phonon thermal Hall effect in insulators.

DOI: 10.1103/PhysRevX.14.041011

Subject Areas: Condensed Matter Physics, Strongly Correlated Materials, Superconductivity

I. INTRODUCTION

The conventional thermal Hall effect describes the appearance of a transverse temperature gradient along the y direction when a heat current J is applied along the x direction and a magnetic field H is applied along the z direction. The thermal Hall effect has become a powerful technique to probe neutral excitations in various quantum materials. It has been shown both theoretically and experimentally that neutral excitations—such as magnons [1,2], phonons [3–11], or even more exotic quasiparticles like Majorana fermions [12,13]—are able to generate a conventional thermal Hall effect.

Recently, the thermal Hall effect measured in a "planar" configuration, i.e., by applying the field inside the xy plane of the sample [as shown in Figs. 1(b) and 1(c)], has been studied in two Kitaev magnets. The first planar thermal Hall effect was observed in the Kitaev candidate material α-$RuCl_3$, where there is still a debate on the existence of a half-quantized thermal Hall conductivity κ_{xy} and on whether the κ_{xy} signal comes from Majorana fermions [14] or chiral magnons [15–17]. A planar thermal Hall effect was also observed in the Kitaev candidate material $Na_2Co_2TeO_6$ [18], where the signal was attributed to chiral magnons.

It has been argued that phonons may in fact be responsible for generating the conventional κ_{xy} measured

*Contact author: lu.chen@usherbrooke.ca
†Contact author: louis.taillefer@usherbrooke.ca

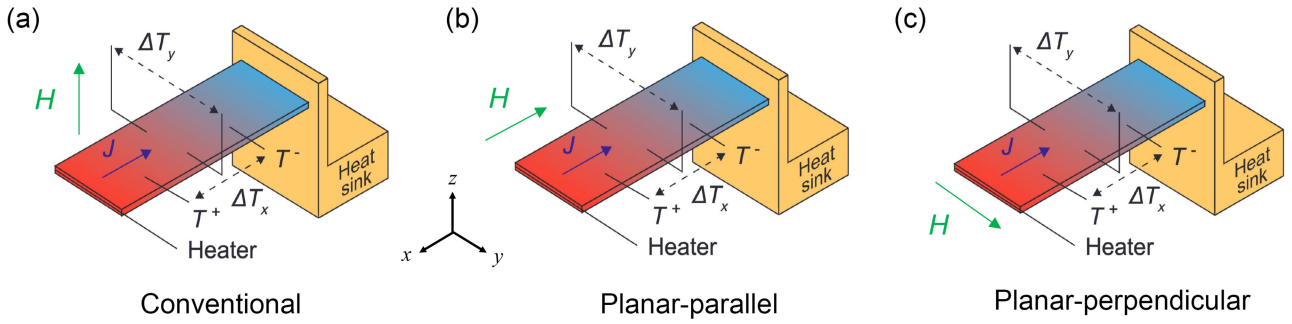

FIG. 1. Schematic of the thermal transport measurement setup. (a) Conventional configuration: $H \parallel z$. (b) Planar-parallel configuration: $H \parallel x$. (c) Planar-perpendicular configuration: $H \parallel y$ (see Sec. II). Directions of both the thermal current J and external magnetic field H are shown with colored arrows. Panel (a) is the configuration for measuring the conventional κ_{xy}. Panels (b) and (c) are for planar κ_{xy}.

in α-$RuCl_3$ and $Na_2Co_2TeO_6$ [19–21]. The question then is whether phonons can also produce a planar κ_{xy}. Here, we address this question by studying the planar κ_{xy} in another family of materials, the cuprates, where the conventional thermal Hall effect has been extensively studied [3–5,7,22]. We report data on the planar κ_{xy} in three different cuprates where the conventional κ_{xy} is dominated by either electrons or phonons. The first is $YBa_2Cu_3O_y$ (YBCO), a superconductor where the conventional κ_{xy} is dominated by electrons [22,23]. We find that the planar κ_{xy} is zero, as expected due to the absence of Lorentz force in a planar-parallel configuration where $H \| J$ [Fig. 1(b)].

The second material is $Nd_{2-x}Ce_xCuO_4$ (NCCO), an insulator at low doping where the conventional κ_{xy} is entirely caused by phonons [7]. Surprisingly, we find a nonzero planar κ_{xy} with a configuration of $H \| J \| a$ of comparable magnitude to the conventional κ_{xy}.

The third cuprate is the superconductor $La_{2-y-x}Eu_ySr_xCuO_4$ (Eu-LSCO) at dopings $p = 0.21$ and 0.24, located on either side of the critical doping $p^\star = 0.23$. It has been shown that a phononic conventional κ_{xy} only exists inside the pseudogap phase, i.e., when $p < p^\star$ [3,4]. We find that the planar κ_{xy} is zero at $p = 0.24$, where the conventional κ_{xy} only comes from electrons. However, the planar κ_{xy} is nonzero at $p = 0.21$, where the conventional κ_{xy} comes from both electrons and phonons. The comparison between Eu-LSCO $p = 0.21$ and 0.24 indicates that the nonzero planar κ_{xy} in $p = 0.21$ is contributed by phonons.

All three cuprates have high crystal symmetries, with YBCO being orthorhombic, and NCCO and Eu-LSCO being tetragonal within the temperature range of the measurement, i.e., below 110 K. In theory, a planar κ_{xy} is not allowed in any of the systems measured here due to their high crystal symmetry [24]. Nevertheless, we observe a sizable planar κ_{xy} coming from phonons, which clearly violates the symmetry requirements. Our results impose a reexamination of the mechanisms responsible for the phonon thermal Hall effect in insulators.

II. METHODS

A. Samples

Our detwinned single crystal of $YBa_2Cu_3O_y$ with $y = 6.54$ was grown at the University of British Columbia by a flux method, as described in Ref. [25]. The hole-doping level $p = 0.11$ is obtained from a superconducting transition temperature $T_c = 60.5$ K. Our single crystal of $Nd_{2-x}Ce_xCuO_4$ with $x = 0.04$ was grown at Stanford University by the traveling-solvent floating-zone method in O_2. Single crystals of $La_{2-y-x}Eu_ySr_xCuO_4$ were grown at the University of Tokyo by the traveling-float-zone technique, with a Eu concentration of $y = 0.2$ and nominal Sr concentration of $x = 0.21$ and 0.24. The hole concentration is given by $p = x$, with an error bar of ± 0.005. The superconducting transition temperature T_c, defined by the zero resistance temperature, is 14 K for Eu-LSCO $x = 0.21$ and 9 K for Eu-LSCO $x = 0.24$. The critical doping level where the pseudogap phase ends in Eu-LSCO is at $p^\star = 0.23$ [26]. A field of 15 T is sufficient to entirely suppress superconductivity in both samples [26].

For the thermal transport measurements, crystals were cut and polished into rectangular platelets with the longest edge along the crystal a axis. Gold contacts were diffused onto the YBCO $p = 0.11$ sample. For NCCO $x = 0.04$, Eu-LSCO $x = 0.21$ and 0.24, contacts were made using silver epoxy, diffused at 500 °C under constant oxygen flow for 1 h. The dimensions (length between contacts $L \times$ width $w \times$ thickness t, in μm) of all the measured samples are listed in Table I.

B. Thermal transport measurements

The thermal conductivity κ_{xx} and thermal Hall conductivity κ_{xy} are measured by applying a heat current J along the x axis of the sample (longest direction) and a magnetic field H either perpendicular to J [$H \| z$ in Fig. 1(a); $H \| y$ in Fig. 1(c)] or parallel to J [$H \| x$, Fig. 1(b)]. Note that $H \| z$ measures the so-called "conventional" thermal Hall effect, while $H \| y$ and $H \| x$ measure the so-called "planar" thermal Hall effect. The heat current J generates a longitudinal

TABLE I. Sample information including the doping level and dimensions of the contacts (length between contacts L × width w × thickness t, in μm).

Material	Doping	L (μm)	w (μm)	t (μm)
$YBa_2Cu_3O_y$	$p = 0.11$	478	784	37
$Nd_{2-x}Ce_xCuO_4$	$x = 0.04$	1209	1232	149
$La_{2-y-x}Eu_ySr_xCuO_4$	$p = 0.21$	652	553	127
$La_{2-y-x}Eu_ySr_xCuO_4$	$p = 0.24$	534	476	168

temperature difference $\Delta T_x = T^+ - T^-$ along the x direction. The thermal conductivity κ_{xx} is defined by

$$\kappa_{xx} = \frac{J}{\Delta T_x}\left(\frac{L}{wt}\right), \tag{1}$$

where w is the sample width, t its thickness, and L the distance between T^+ and T^-. When a magnetic field is applied along either the x, y, or z direction, a transverse temperature difference ΔT_y can be measured along the y axis. The thermal Hall conductivity κ_{xy} is then given by

$$\kappa_{xy} = -\kappa_{yy}\left(\frac{\Delta T_y}{\Delta T_x}\right)\left(\frac{L}{w}\right). \tag{2}$$

In a tetragonal system, such as NCCO and Eu-LSCO, we can take $\kappa_{yy} = \kappa_{xx}$ at $H = 0$ T. However, with a magnetic field applied in the xy plane, the rotational symmetry is broken even for tetragonal structures. As shown in Eq. (2), to calculate κ_{xy} with $H\|x$, we need to use κ_{yy} measured with $H\|x$, instead of using κ_{yy} measured with $H\|y$. This method requires another sample with the geometry and configuration of $J\|y$ prepared separately (more details can be found in Ref. [24]); then, κ_{xy} can be calculated accordingly. In this study, for NCCO and Eu-LSCO, we use κ_{yy} measured with $H\|y$ in the same sample to approximate the κ_{yy} measured with $H\|x$ that is supposed to be taken in a separate sample. The resulting error on the true κ_{xy} value can be estimated to be less than 8% based on the value of κ_{xx}, with different in-plane field directions as shown in Fig. 3(b). In an orthorhombic system like YBCO, κ_{yy} is measured in a separate sample with the heat current along the y direction [22].

Both thermal conductivity κ_{xx} and thermal Hall conductivity κ_{xy} are measured with a steady-state method. The thermal gradient along the sample is provided by a resistive heater connected to one end of the sample. The other end of the sample is glued to a heat sink with silver paint. The longitudinal and transverse temperature differences ΔT_x and ΔT_y are measured using type-E thermocouples. All the measurements are carried out in a standard variable temperature insert (VTI) system up to 15 T.

The measurement procedure is the following: A magnetic field of $+H$ is applied at $T = 90$ K; then, the sample is cooled down with the $+H$ field to the base temperature (around 2–3 K). The $+H$ data are taken by changing the temperature in discrete steps at a fixed magnetic field during the warm-up process. After the $+H$ data are taken, a magnetic field of $-H$ is applied at the same temperature of $T = 90$ K; then, the sample is cooled with the $-H$ field down to base temperature. The $-H$ data are taken by the same method during the warm-up process. During the measurement, after the temperature is stabilized at each step, the background of the thermocouple is eliminated by subtracting the heater-off value from the heater-on value. The contamination from κ_{xx} in κ_{xy} due to contact misalignment is removed by field antisymmetrization of the transverse temperature difference ΔT_y. In other words, ΔT_y is measured with both positive and negative magnetic fields in the same conditions; then, κ_{xy} is calculated using the field antisymmetrized ΔT_y, i.e., $\Delta T_y(H) = [\Delta T_y(T,H) - \Delta T_y(T,-H)]/2$. The misalignment angle between the sample and the external magnetic field is within 1 to 2 degrees. We have tested different measurement procedures, i.e., temperature steps at fixed fields vs field steps at fixed temperatures, and found that they produce equivalent results [27]. More details regarding the technique can be found in Refs. [4,5,22].

In a planar configuration, there is no convention for the sign of the Hall signal, unlike in the case of the conventional thermal Hall effect. To define a sign for ΔT_y, we need to know whether the left side of the sample is hotter or colder than the right side. In the conventional configuration ($H\|z$), left and right can be defined (as with the Lorentz force). However, in the case where $H\|J$, it is not possible to define left and right since the plane of the sample is parallel to the CuO_2 planes of the crystal, which is a mirror plane. Thus, in our figures, the planar thermal Hall data are presented in their absolute value, $|\kappa_{xy}|$ or $-|\kappa_{xy}|$, for convenience of comparison. The point here is to compare the absolute value of the planar Hall effect to that of the conventional Hall effect.

III. RESULTS

A. YBCO $p = 0.11$

First, we measured the planar κ_{xy} in YBCO $p = 0.11$, which is an underdoped cuprate superconductor with $T_c = 60.5$ K [see Fig. 2(a)]. The conventional thermal Hall conductivity κ_{xy} measured in one sample with a configuration of $J\|b$, $H\|c$ at $H = 1$ T is plotted in Fig. 2(b) (blue circles) and the ratio $|\kappa_{xy}/\kappa_{xx}|$ in Fig. 2(c). The huge increase in κ_{xy} below T_c comes from an enhancement of the electronic mean free path due to the loss of inelastic scattering as electrons condense into Cooper pairs, in clean crystals where the elastic scattering due to disorder is very small [23]. The κ_{xy} signal in this conventional configuration ($H\|c$) is completely dominated by electrons

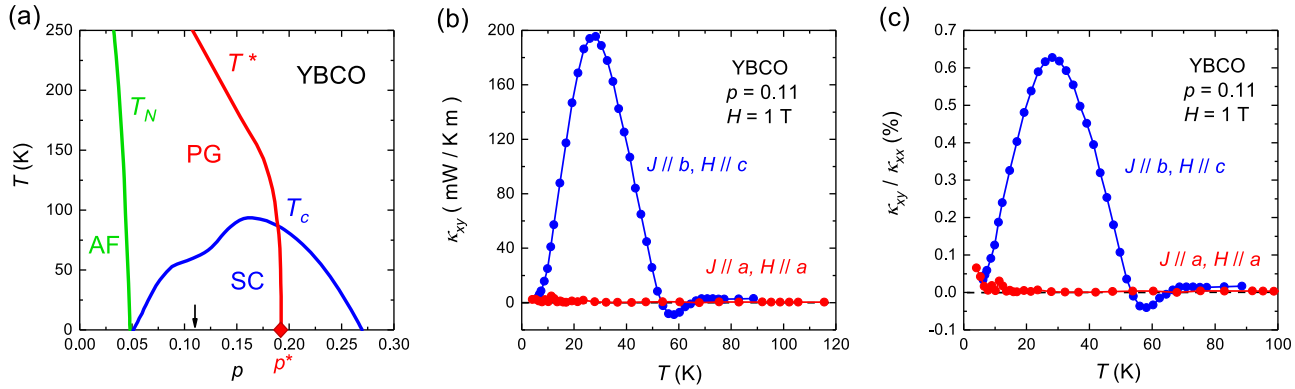

FIG. 2. (a) Schematic temperature-doping phase diagram of the hole-doped cuprate YBCO. The antiferromagnetic (AF) phase is delineated by the Néel temperature T_N (green line). The superconducting phase (SC) is bounded by the zero-field critical temperature T_c (blue line). The pseudogap (PG) phase is bounded by the critical temperature $T^\star$ (red line) and critical doping $p^\star = 0.19$ (red diamond). The black arrow marks the doping level of the sample measured in this study ($p = 0.11$). Panel (a) is replotted from Fig. 1(a) in Ref. [28]. (b) Thermal Hall conductivity and (c) thermal Hall angle for YBCO $p = 0.11$ measured at $H = 1$ T, plotted as κ_{xy} vs T and κ_{xy}/κ_{xx} vs T. The blue circles show κ_{xy} measured in the conventional configuration of $J\|b$, $H\|c$; its sign obeys the usual convention. The red circles show κ_{xy} measured in the planar configuration of $H\|J\|a$ plotted as its absolute value $|\kappa_{xy}|$. Compared to the large conventional κ_{xy} signal, the planar κ_{xy} is zero at the same field. Lines are a guide to the eye.

(more specifically, d-wave quasiparticles), and these electrons respond to the Lorentz force (given that $H\perp J$).

In a second sample cut from the same mother YBCO crystal, we performed the same measurement of κ_{xy} but with the field applied parallel to the current ($H\|J\|a$). The data measured also at $H = 1$ T are shown in Fig. 2(b) and 2(c) (red circles). We see that $\kappa_{xy} = 0$, as expected since there is no Lorentz force acting on the electrons (given that $H\|J$). Thus, electrons indeed do not generate a planar-parallel Hall effect, at least in this orthorhombic cuprate. This measurement also demonstrates that our method for detecting a planar κ_{xy} is reliable to a high accuracy.

B. NCCO $x = 0.04$

Next, we turn to the AF insulating cuprate NCCO at a doping $x = 0.04$ [Fig. 3(a)], where a large conventional κ_{xy} contributed by phonons was reported before [7]. The conventional κ_{xy} in NCCO $x = 0.04$ is attributed to phonons for the following reasons. First, electronic conduction is negligible in this nearly insulating sample. Second, $\kappa_{xy}(T)$ displays a temperature dependence that closely mimics that of the phonon-dominated $\kappa_{xx}(T)$. Third, when applying the heat current along the c axis (and magnetic field along the a axis), the thermal Hall angle κ_{zy}/κ_{zz} shows a comparable magnitude to κ_{xy}/κ_{xx}, i.e., on the order of about 1%. When the heat current is applied perpendicular to the CuO_2 plane (along the c axis), the only heat carriers that can propagate along the c axis are phonons since magnons are confined inside the CuO_2 planes. Thus, the c-axis thermal Hall conductivity κ_{zy} is purely contributed by phonons. A similar thermal Hall angle between κ_{xy} and κ_{zy} indicates that κ_{xy} is also contributed by phonons.

The temperature-dependent thermal conductivity κ_{xx} measured with $J\|a$ at $H = 15$ T for three different field directions is plotted in Fig. 3(b). Note that κ_{xx} shows a strong dependence on the field direction, as has been observed in the mother compound Nd_2CuO_4 [29]. As shown in Fig. 3(c), the conventional κ_{xy} taken with $J\|a$, $H\|c$ at $H = 15$ T (blue curve) shows a temperature-dependent negative signal, which is the typical behavior of the phononic κ_{xy} observed in both hole-doped and electron-doped cuprates [3,4,7]. The planar κ_{xy} measured in the same sample with a configuration of $H\|J\|a$ (red curve) and $J\|a$, $H\|b$ (green curve) is shown in Fig. 3(c). The planar-parallel κ_{xy} taken with $H\|J\|a$ at $H = 15$ T (red curve) is nonzero and shows a comparable magnitude to the conventional κ_{xy}. For a field in the plane but perpendicular to the current ($H\|$ b), a nonzero planar-perpendicular κ_{xy} signal is also observed [green curve in Fig. 3(c)]. The planar κ_{xy} measured in both configurations not only follows the same temperature dependence as the κ_{xx} signal taken simultaneously but also peaks at the same temperature as κ_{xx}. This concomitant behavior between κ_{xy} and κ_{xx} confirms a phononic origin for the planar κ_{xy} in NCCO $x = 0.04$. The corresponding thermal Hall angle κ_{xy}/κ_{xx} measured with three different field directions is plotted in Fig. 3(d).

C. Eu-LSCO $p = 0.21$ and 0.24

After studying the planar κ_{xy} in materials where the conventional κ_{xy} is either dominated by electrons (YBCO $p = 0.11$) or by phonons (NCCO $x = 0.04$), we turn to the third cuprate material, Eu-LSCO, where the phononic conventional κ_{xy} can be switched on and off by changing the doping level. It was shown in a previous study [3,4] that

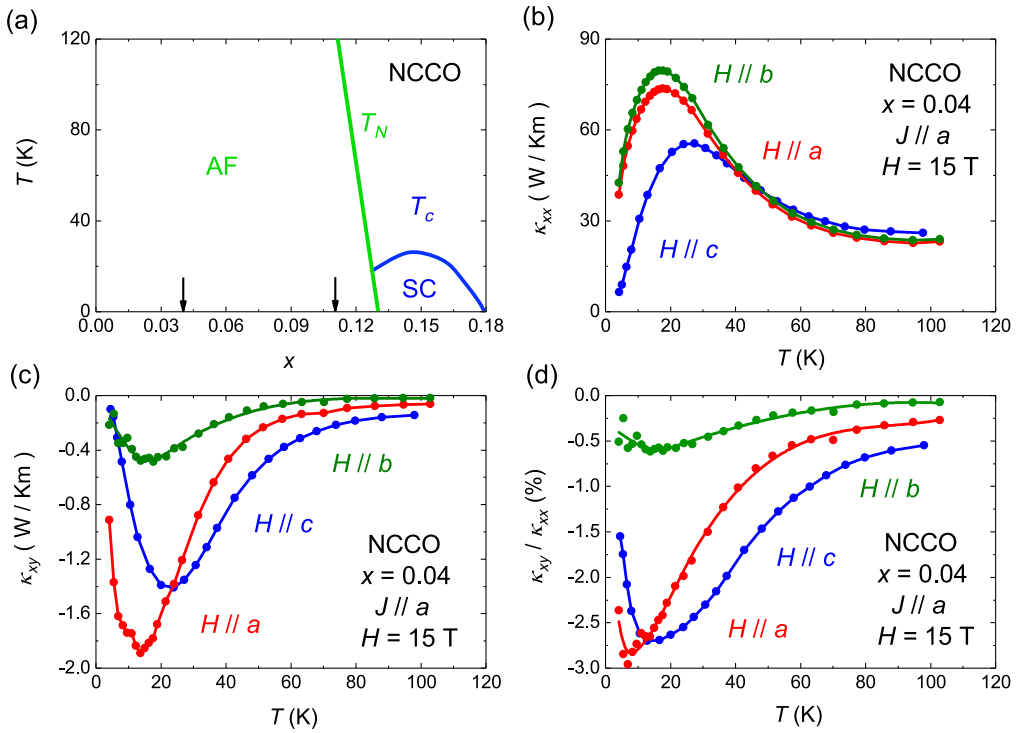

FIG. 3. (a) Schematic temperature-doping phase diagram of the electron-doped cuprate NCCO. The AF phase is delineated by the Néel temperature T_N (green line). The superconducting (SC) phase is bounded by the zero-field critical temperature T_c (blue line). The black arrows mark the doping levels of the samples measured in this study, $x = 0.04$ and 0.11. The $x = 0.11$ data are presented in the Appendix. Panel (a) is replotted from Fig. 1 in Ref. [7]. (b) Thermal conductivity, (c) thermal Hall conductivity, and (d) thermal Hall angle for NCCO $x = 0.04$ measured at $H = 15$ T, and plotted as κ_{xx} vs T, κ_{xy} vs T, and κ_{xy}/κ_{xx} vs T. Note that κ_{xx} and κ_{xy} measured in the conventional configuration of $J\|a$, $H\|c$ (blue) are taken from Ref. [7], and κ_{xx} and κ_{xy} measured in the planar configuration of $H\|J\|a$ ($J\|a$, $H\|b$) are plotted as κ_{xx} and $-|\kappa_{xy}|$ and marked in red (green). The magnitude of the planar-parallel κ_{xy} ($H\|J\|a$) is comparable to the conventional κ_{xy}. Lines are a guide to the eye.

the conventional κ_{xy} in the hole-doped cuprates Nd-LSCO and Eu-LSCO comes from both electrons and phonons inside the pseudogap phase, while it only comes from electrons when the doping level exceeds the pseudogap critical doping $p^\star$. The phononic origin of the conventional κ_{xy} in Eu-LSCO and Nd-LSCO inside the pseudogap phase is established in the following way. When applying the heat current along the c axis (and magnetic field along the a axis), κ_{zy} is zero at $p = 0.24$ while κ_{zy} shows a large negative signal at $p = 0.21$ [4]. Since magnons are highly confined inside the CuO_2 planes and the electron contribution to κ_{zy} is negligible according to the Wiedemann-Franz Law, κ_{zy} is only contributed by phonons. These sets of experiments indicate that the conventional κ_{zy} is purely contributed by phonons and only nonzero inside the pseudogap phase. When looking back at κ_{xy}, the nonzero conventional κ_{xy} signal at $p = 0.24$ comes only from electrons [Fig. 4(b); blue curve], while at $p = 0.21$ it is dominated by the positive electronic contribution at high temperature and the negative phononic contribution at low temperature [Fig. 4(c); blue curve].

The two Eu-LSCO samples measured in this study are $p = 0.21$ and $p = 0.24$, respectively located on each side of $p^\star = 0.23$ [Fig. 4(a)]. In Eu-LSCO $p = 0.24$, the conventional κ_{xy} taken with $J\|a$, $H\|c$ at $H = 15$ T is plotted as the blue curve in Fig. 4(b), which is positive and only contributed by electrons. The planar κ_{xy} measured in the same sample with $H\|J\|a$ shows a zero signal (red curve). This result again shows that in a material where the conventional κ_{xy} comes only from electrons, the planar κ_{xy} signal is zero, in agreement with what we found in YBCO $p = 0.11$. In this tetragonal cuprate, there is no planar-parallel κ_{xy} signal. This second measurement also confirms that our method for detecting a planar κ_{xy} is reliable, this time in a field as large as 15 T.

In Eu-LSCO $p = 0.21$, the conventional κ_{xy} taken with $J\|a$, $H\|c$ at $H = 15$ T is plotted as the blue curve in Fig. 4(c). We see that it is dominated by the positive electronic κ_{xy} at high temperature and the negative phononic κ_{xy} at low temperature. The planar κ_{xy} measured in the same sample with $H\|J\|a$ shows a nonzero signal (red curve), which grows upon cooling in tandem with the emergence of the phononic conventional κ_{xy}. We conclude that, in this tetragonal cuprate, a planar-parallel κ_{xy} signal appears, and it is associated with phonons.

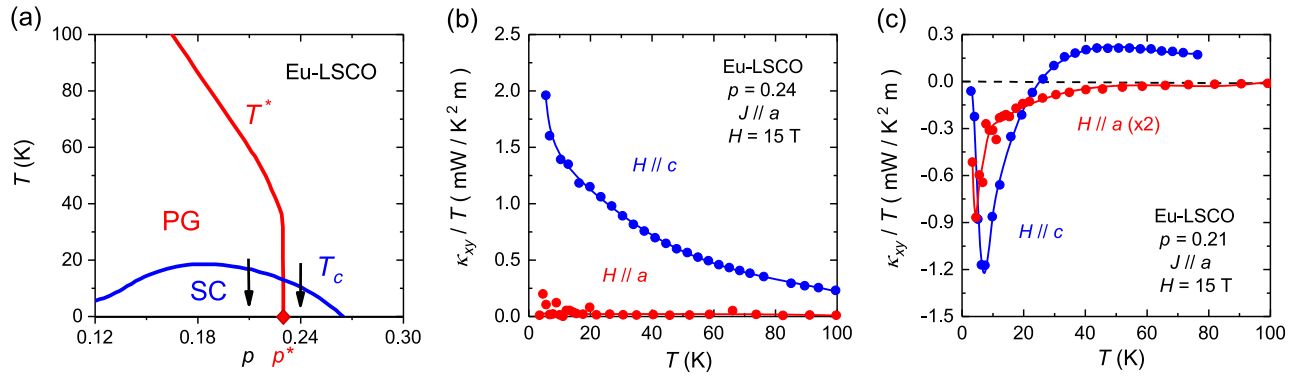

FIG. 4. (a) Schematic temperature-doping phase diagram of the hole-doped cuprate Eu-LSCO. The superconducting (SC) phase is bounded by the zero-field critical temperature T_c (blue line). The pseudogap phase (PG) is bounded by the critical temperature $T^\star$ (red line), which ends at the critical doping $p^\star = 0.23$ (red diamond). The black arrows mark the doping levels of the two Eu-LSCO samples measured in this study, at $p = 0.21$ and 0.24. Panel (a) is replotted from Fig. 2(a) in Ref. [4]. Thermal Hall conductivity for Eu-LSCO at (b) $p = 0.24$ and (c) $p = 0.21$, measured at $H = 15$ T, plotted as κ_{xy}/T vs T. Note that κ_{xy} measured in the conventional configuration of $J\|a$, $H\|c$ (blue) is taken from Ref. [3]. The conventional κ_{xy} contains both a positive electron contribution and a negative phonon contribution at $p = 0.21$ while it is purely contributed by electrons at $p = 0.24$, outside the pseudogap phase [4]. Here, κ_{xy} measured in the planar-parallel configuration of $H\|J\|a$ is plotted as its absolute value $|\kappa_{xy}|$ for $p = 0.24$ [panel (b)] and as $-|\kappa_{xy}|$ for $p = 0.21$ [panel (c)], minus sign for convenience, both marked in red. The planar κ_{xy} is zero at $p = 0.24$, where only electrons generate a Hall response, whereas it is nonzero at $p = 0.21$, when phonons contribute. Lines are a guide to the eye.

IV. DISCUSSION

Our results in YBCO $p = 0.11$ at $H = 1$ T and Eu-LSCO $p = 0.24$ at $H = 15$ T show that the planar κ_{xy} coming from electrons is zero in cuprates, as expected since electrons feel zero Lorentz force when the magnetic field is parallel to the heat current ($H\|J$). These two sets of experiments also establish that our measurement procedure is reliable; i.e., field antisymmetrization on ΔT_y between $+H$ and $-H$ runs gives the expected result.

Our results in NCCO $x = 0.04$ and Eu-LSCO $p = 0.21$ clearly show that phonons are able to generate a sizable planar thermal Hall signal. The question is how to reconcile our results with the symmetry requirements? Theories point out that, in order to have a nonzero planar κ_{xy}, certain symmetry requirements have to be fulfilled to make $H\|J$ different from $H\| - J$ [14,16,17,24]. However, we observe a nonzero planar κ_{xy} in two tetragonal systems, NCCO and Eu-LSCO (space group I4/mmm), which clearly violates the symmetry requirements.

Our speculation is that a nonzero planar κ_{xy} signal could potentially result from a locally broken symmetry due to impurities, defects, or domains. A possible mechanism for NCCO, an AF insulator with $T_N \sim 200$ K, is the scattering of phonons by antiferromagnetic domains. This mechanism is reminiscent of the nonmagnetic insulator $SrTiO_3$, where the conventional κ_{xy} was attributed to the scattering of phonons by antiferrodistortive structural domains [6,30]. In cuprates, disorder coming from dopants and oxygen vacancies could also be the source of local symmetry breaking [7]. This type of extrinsic mechanism could potentially work for both conventional and planar configurations of the phonon thermal Hall effect.

Our findings call for a reevaluation of the previously reported results in the Kitaev candidate materials. In α-$RuCl_3$, a nonzero planar κ_{xy} was only observed with a configuration of $H\|J\|a$ but not with $H\|J\|b$ [31] due to the fact that the C_2 rotational symmetry is preserved only along the b axis and not along the a axis [14–17]. This explanation is based on the symmetry properties of the monoclinic structure in the $C2/m$ space group. However, three different low-temperature structures have been reported for α-$RuCl_3$: monoclinic $C2/m$ [32,33], trigonal $P3_112$ [34], and rhombohedral $R\bar{3}$ [35]. This controversy could potentially change the symmetry argument for the planar κ_{xy} data. Furthermore, the thermal transport properties have been reported to highly depend on the stacking disorder in the samples, which results from different growth techniques and handling processes [36,37]. In $Na_2Co_2TeO_6$ (space group $P6_322$), a nonzero planar κ_{xy} has been observed along both the zigzag and armchair directions [18], which are, in principle, both forbidden since the crystal structure has C_2 rotational symmetry along both directions. The observation of a planar κ_{xy} in $Na_2Co_2TeO_6$ points to an extrinsic mechanism that can locally break the symmetry.

Note that, in addition to cuprates, we have also observed a phononic planar thermal Hall signal (comparable in magnitude to the conventional thermal Hall signal) in the Kitaev magnet $Na_2Co_2TeO_6$ [38] and in the frustrated antiferromagnetic insulator Y-kapellasite [39], thereby further validating the existence of a planar thermal Hall signal coming from phonons.

Very recently, a planar thermal Hall signal was also reported in three other insulators, $SrTiO_3$, SiO_2, and black phosphorous by Jin *et al.* [40] and Li *et al.* [41], where, in all cases, it is attributed to phonons. These three insulators have a high crystal symmetry for which a planar thermal Hall effect should, in theory, be forbidden.

V. CONCLUSION

We report a systematic study of the planar thermal Hall response in three cuprate materials. In orthorhombic YBCO (at $p = 0.11$), the large electronic κ_{xy} observed in the conventional configuration ($H\|c$) disappears entirely when the field is applied parallel to the current ($H\|a$), as expected in the absence of a Lorentz force when $H\|J$. In tetragonal Eu-LSCO at $p = 0.24$, where the conventional κ_{xy} is entirely electronic, we also find a zero Hall signal in the planar configuration ($H\|J\|a$). In dramatic contrast, we observe a planar Hall response that is as large as the conventional Hall response in the tetragonal cuprate NCCO (at $x = 0.04$), an insulator in which the Hall response is entirely due to phonons. We conclude that phonons can produce a planar thermal Hall effect even in materials where it is forbidden by global symmetry. We propose that the planar thermal Hall signal emerges from a local symmetry breaking, presumably associated with impurities, defects, or domains. Our work reveals an entirely new facet of the phonon thermal Hall effect, namely, that it can also occur in a planar configuration. This new observation indicates that the direction of the external magnetic field does not matter much in the case of the phonon κ_{xy}. Whatever mechanism governs the phonon κ_{xy} in a conventional configuration should also be responsible for it in a planar configuration. Our findings call for a complete reexamination of the mechanism responsible for a phonon thermal Hall effect in insulators and also a reevaluation of the planar thermal Hall conductivity reported in Kitaev candidate materials.

ACKNOWLEDGMENTS

We thank K. Behnia, H. Y. Guo, H. Y. Kim, S. A. Kivelson, and R. Valenti for fruitful discussions. We thank S. Fortier for his assistance with the experiments. L. T. acknowledges support from the Canadian Institute for Advanced Research (CIFAR) as a CIFAR Fellow and funding from the Institut Quantique, the Natural Sciences and Engineering Research Council of Canada (Grant No. PIN:123817), the Fonds de Recherche du Québec—Nature et Technologies, the Canada Foundation for Innovation, and a Canada Research Chair. This research was undertaken thanks, in part, to funding from the Canada First Research Excellence Fund. Z-X. S. acknowledges the support of the U.S. Department of Energy, Office of Science, Office of Basic Energy Sciences, Division of Material Sciences and Engineering, under Contract No. DE-AC02-76SF00515. G. G. acknowledges support from the ANR Grants STeP2 No. ANR-22-EXES-0013; 318 QuantExt No. ANR-23-CE30-0001-01; and the France 2030 Program No. ANR-24-RRII-0004.

APPENDIX: NCCO $x = 0.11$

To explore the doping dependence of the planar thermal Hall effect generated by phonons in cuprates, we investigated the electron-doped cuprate $Nd_{2-x}Ce_xCuO_4$ at two dopings, $x = 0.04$ and $x = 0.11$, both inside the antiferromagnetic ordered insulating phase [Fig. 3(a)]. In Fig. 5(b), we show the thermal Hall conductivity κ_{xy} of $Nd_{2-x}Ce_xCuO_4$ at $x = 0.11$, taken in three different configurations. When comparing to the data taken in $Nd_{2-x}Ce_xCuO_4$ at $x = 0.04$ (Fig. 3), we see that the conventional κ_{xy} (blue) is comparable at these two doping levels, in both magnitude and T dependence. However, the planar κ_{xy} is much smaller in the $x = 0.11$ sample, especially in the planar-parallel configuration (red). This finding indicates that the planar κ_{xy} is either strongly sample dependent or strongly doping dependent.

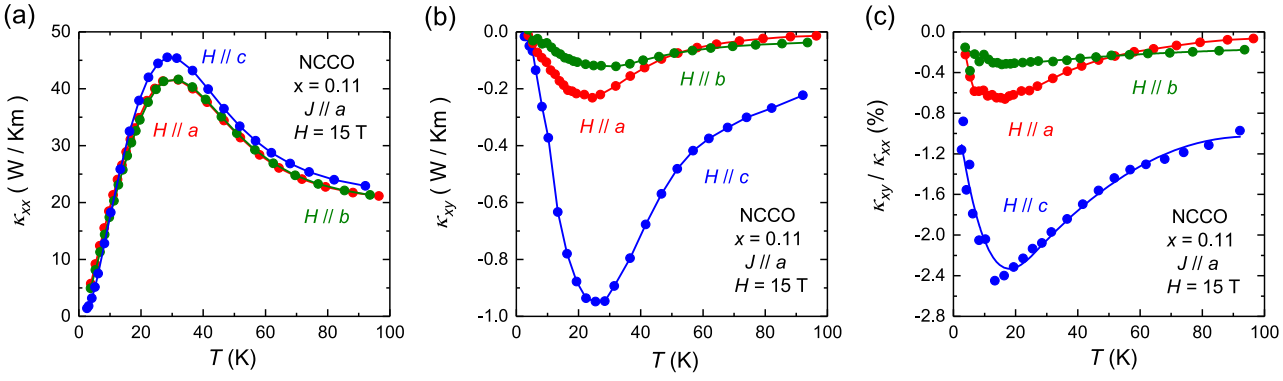

FIG. 5. (a) Thermal conductivity, (b) thermal Hall conductivity, and (c) thermal Hall angle for NCCO $x = 0.11$ measured at $H = 15$ T, plotted as κ_{xx} vs T, κ_{xy} vs T, and κ_{xy}/κ_{xx} vs T. Note that κ_{xx} and κ_{xy} measured in the conventional configuration of $J\|a$, $H\|c$ (blue) are taken from Ref. [7]; κ_{xx} and κ_{xy} measured in the planar configuration of $H\|J\|a$ ($J\|a$, $H\|b$) are plotted as κ_{xx} and $-|\kappa_{xy}|$ and marked in red (green). Lines are a guide to the eye.

[1] Y. Onose, T. Ideue, H. Katsura, Y. Shiomi, N. Nagaosa, and Y. Tokura, *Observation of the magnon Hall effect*, Science **329**, 297 (2010).

[2] H. Katsura, N. Nagaosa, and P. A. Lee, *Theory of the thermal Hall effect in quantum magnets*, Phys. Rev. Lett. **104**, 066403 (2010).

[3] G. Grissonnanche, A. Legros, S. Badoux, E. Lefrançois, M. L. V. Zatko, F. Laliberté, A. Gourgout, J.-S. Zhou, S. Pyon, T. Takayama, H. Takagi, S. Ono, N. Doiron-Leyraud, and L. Taillefer, *Giant thermal Hall conductivity in the pseudogap phase of cuprate superconductors*, Nature (London) **571**, 376 (2019).

[4] G. Grissonnanche, S. Thériault, A. Gourgout, M.-E. Boulanger, E. Lefrançois, A. Ataei, F. Laliberté, M. Dion, J.-S. Zhou, S. Pyon, T. Takayama, H. Takagi, N. Doiron-Leyraud, and L. Taillefer, *Chiral phonons in the pseudogap phase of cuprates*, Nat. Phys. **16**, 1108 (2020).

[5] M.-E. Boulanger, G. Grissonnanche, S. Badoux, A. Allaire, E. Lefrançois, A. Legros, A. Gourgout, M. Dion, C. H. Wang, X. H. Chen, R. Liang, W. N. Hardy, D. A. Bonn, and L. Taillefer, *Thermal Hall conductivity in the cuprate Mott insulators* Nd_2CuO_4 *and* $Sr_2CuO_2Cl_2$, Nat. Commun. **11**, 5325 (2020).

[6] X. Li, B. Fauqué, Z. Zhu, and K. Behnia, Phonon thermal Hall effect in strontium titanate, Phys. Rev. Lett. **124**, 105901 (2020).

[7] M.-E. Boulanger, G. Grissonnanche, E. Lefrançois, A. Gourgout, K.-J. Xu, Z.-X. Shen, R. L. Greene, and L. Taillefer, *Thermal Hall conductivity of electron-doped cuprates*, Phys. Rev. B **105**, 115101 (2022).

[8] L. Chen, M.-E. Boulanger, Z.-C. Wang, F. Tafti, and L. Taillefer, *Large phonon thermal Hall conductivity in the antiferromagnetic insulator* Cu_3TeO_6, Proc. Natl. Acad. Sci. U.S.A. **119**, e2208016119 (2022).

[9] T. Uehara, T. Ohtsuki, M. Udagawa, S. Nakatsuji, and Y. Machida, *Phonon thermal Hall effect in a metallic spin ice*, Nat. Commun. **13**, 4604 (2022).

[10] X. Li, Y. Machida, A. Subedi, Z. Zhu, L. Li, and K. Behnia, *The phonon thermal Hall angle in black phosphorus*, Nat. Commun. **14**, 1027 (2023).

[11] A. Ataei, G. Grissonnanche, M.-E. Boulanger, L. Chen, E. Lefrançois, V. Brouet, and L. Taillefer, *Phonon chirality from impurity scattering in the antiferromagnetic phase of* Sr_2IrO_4, Nat. Phys. **20**, 585 (2024).

[12] Y. Kasahara, T. Ohnishi, Y. Mizukami, O. Tanaka, S. Ma, K. Sugii, N. Kurita, H. Tanaka, J. Nasu, Y. Motome, T. Shibauchi, and Y. Matsuda, *Majorana quantization and half-integer thermal quantum Hall effect in a Kitaev spin liquid*, Nature (London) **559**, 227 (2018).

[13] J. A. N. Bruin, R. R. Claus, Y. Matsumoto, N. Kurita, H. Tanaka, and H. Takagi, *Robustness of the thermal Hall effect close to half-quantization in* α-$RuCl_3$, Nat. Phys. **18**, 401 (2022).

[14] T. Yokoi, S. Ma, Y. Kasahara, S. Kasahara, T. Shibauchi, N. Kurita, H. Tanaka, J. Nasu, Y. Motome, C. Hickey, S. Trebst, and Y. Matsuda, *Half-integer quantized anomalous thermal Hall effect in the Kitaev material candidate* α-$RuCl_3$, Science **373**, 568 (2021).

[15] P. Czajka, T. Gao, M. Hirschberger, P. Lampen-Kelley, A. Banerjee, N. Quirk, D. G. Mandrus, S. E. Nagler, and N. P. Ong, *Planar thermal Hall effect of topological bosons in the Kitaev magnet* α-$RuCl_3$, Nat. Mater. **22**, 36 (2023).

[16] L. E. Chern, E. Z. Zhang, and Y. B. Kim, *Sign structure of thermal Hall conductivity and topological magnons for in-plane field polarized Kitaev magnets*, Phys. Rev. Lett. **126**, 147201 (2021).

[17] E. Z. Zhang, L. E. Chern, and Y. B. Kim, *Topological magnons for thermal Hall transport in frustrated magnets with bond-dependent interactions*, Phys. Rev. B **103**, 174402 (2021).

[18] H. Takeda, J. Mai, M. Akazawa, K. Tamura, J. Yan, K. Moovendaran, K. Raju, R. Sankar, K.-Y. Choi, and M. Yamashita, *Planar thermal Hall effects in the Kitaev spin liquid candidate* $Na_2Co_2TeO_6$, Phys. Rev. Res. **4**, L042035 (2022).

[19] E. Lefrançois, G. Grissonnanche, J. Baglo, P. Lampen-Kelley, J.-Q. Yan, C. Balz, D. Mandrus, S. E. Nagler, S. Kim, Y.-J. Kim, N. Doiron-Leyraud, and L. Taillefer, *Evidence of a phonon Hall effect in the Kitaev spin liquid candidate* α-$RuCl_3$, Phys. Rev. X **12**, 021025 (2022).

[20] M. Gillig, X. Hong, C. Wellm, V. Kataev, W. Yao, Y. Li, B. Büchner, and C. Hess, *Phononic-magnetic dichotomy of the thermal Hall effect in the Kitaev-Heisenberg candidate material* $Na_2Co_2TeO_6$, Phys. Rev. Res. **5**, 043110 (2023).

[21] H. Yang, C. Kim, Y. Choi, J. H. Lee, G. Lin, J. Ma, M. Kratochvílová, P. Proschek, E.-G. Moon, K. H. Lee, Y. S. Oh, and J.-G. Park, *Significant thermal Hall effect in* 3*d cobalt Kitaev system* $Na_2Co_2TeO_6$, Phys. Rev. B **106**, L081116 (2022).

[22] G. Grissonnanche, F. Laliberté, S. Dufour-Beauséjour, M. Matusiak, S. Badoux, F. F. Tafti, B. Michon, A. Riopel, O. Cyr-Choinière, J. C. Baglo, B. J. Ramshaw, R. Liang, D. A. Bonn, W. N. Hardy, S. Krämer, D. LeBoeuf, D. Graf, N. Doiron-Leyraud, and L. Taillefer, *Wiedemann-Franz law in the underdoped cuprate superconductor* $YBa_2Cu_3O_y$, Phys. Rev. B **93**, 064513 (2016).

[23] Y. Zhang, N. P. Ong, P. W. Anderson, D. A. Bonn, R. Liang, and W. N. Hardy, *Giant enhancement of the thermal Hall conductivity* κ_{xy} *in the superconductor* $YBa_2Cu_3O_{6.95}$, Phys. Rev. Lett. **86**, 890 (2001).

[24] T. Kurumaji, *Symmetry-based requirement for the measurement of electrical and thermal Hall conductivity under an in-plane magnetic field*, Phys. Rev. Res. **5**, 023138 (2023).

[25] R. Liang, D. Bonn, and W. N. Hardy, *Evaluation of* CuO_2 *plane hole doping in* $YBa_2Cu_3O_{6+x}$ *single crystals*, Phys. Rev. B **73**, 180505(R) (2006).

[26] B. Michon, C. Girod, S. Badoux, J. Kačmarčík, Q. Ma, M. Dragomir, H. A. Dabkowska, B. D. Gaulin, J.-S. Zhou, S. Pyon, T. Takayama, H. Takagi, S. Verret, N. Doiron-Leyraud, C. Marcenat, L. Taillefer, and T. Klein, *Thermodynamic signatures of quantum criticality in cuprate superconductors*, Nature (London) **567**, 218 (2019).

[27] A. Vallipuram, L. Chen, E. Campillo, M. Mezidi, G. Grissonnanche, M.-E. Boulanger, E. Lefrançois, M. P. Zic, Y. Li, I. R. Fisher, J. Baglo, and L. Taillefer, *Role of magnetic ions in the thermal Hall effect of the paramagnetic insulator* $TmVO_4$, Phys. Rev. B **110**, 045144 (2024).

[28] C. Proust and L. Taillefer, *The remarkable underlying ground states of cuprate superconductors*, Annu. Rev. Condens. Matter Phys. **10**, 409 (2019).

[29] S. Y. Li, L. Taillefer, C. H. Wang, and X. H. Chen, *Ballistic magnon transport and phonon scattering in the antiferromagnet* Nd_2CuO_4, Phys. Rev. Lett. **95**, 156603 (2005).

[30] J.-Y. Chen, S. A. Kivelson, and X.-Q. Sun, *Enhanced thermal Hall effect in nearly ferroelectric insulators*, Phys. Rev. Lett. **124**, 167601 (2020).

[31] P. Czajka, T. Gao, M. Hirschberger, P. Lampen-Kelley, A. Banerjee, J. Yan, D. G. Mandrus, S. E. Nagler, and N. P. Ong, *Oscillations of the thermal conductivity in the spin-liquid state of* α-$RuCl_3$, Nat. Phys. **17**, 915 (2021).

[32] R. D. Johnson, S. C. Williams, A. A. Haghighirad, J. Singleton, V. Zapf, P. Manuel, I. I. Mazin, Y. Li, H. O. Jeschke, R. Valentí, and R. Coldea, *Monoclinic crystal structure of* α-$RuCl_3$ *and the zigzag antiferromagnetic ground state*, Phys. Rev. B **92**, 235119 (2015).

[33] H. B. Cao, A. Banerjee, J.-Q. Yan, C. A. Bridges, M. D. Lumsden, D. G. Mandrus, D. A. Tennant, B. C. Chakoumakos, and S. E. Nagler, *Low-temperature crystal and magnetic structure of* α-$RuCl_3$, Phys. Rev. B **93**, 134423 (2016).

[34] K. W. Plumb, J. P. Clancy, L. J. Sandilands, V. Vijay Shankar, Y. F. Hu, K. S. Burch, H.-Y. Kee, and Y.-J. Kim, α-$RuCl_3$*: A spin-orbit assisted Mott insulator on a honeycomb lattice*, Phys. Rev. B **90**, 041112(R) (2014).

[35] A. Glamazda, P. Lemmens, S.-H. Do, Y. S. Kwon, and K.-Y. Choi, *Relation between Kitaev magnetism and structure in* α-$RuCl_3$, Phys. Rev. B **95**, 174429 (2017).

[36] H. Zhang, A. May, H. Miao, B. Sales, D. Mandrus, S. Nagler, M. McGuire, and J. Yan, *Sample-dependent and sample-independent thermal transport properties of* α-$RuCl_3$, Phys. Rev. Mater. **7**, 114403 (2023).

[37] H. Zhang, M. A. McGuire, A. F. May, J. Chao, Q. Zheng, M. Chi, B. C. Sales, D. G. Mandrus, S. E. Nagler, H. Miao, F. Ye, and J. Yan, *Stacking disorder and thermal transport properties of* α-$RuCl_3$, Phys. Rev. Mater. **8**, 014402 (2024).

[38] L. Chen, E. Lefrançois, A. Vallipuram, Q. Barthélemy, A. Ataei, W. Yao, Y. Li, and L. Taillefer, *Planar thermal Hall effect from phonons in a Kitaev candidate material*, Nat. Commun. **15**, 3513 (2024).

[39] Q. Barthélemy, E. Lefrançois, P. Puphal, K. M. Zoch, L. Chen, A. Vallipuram, C. Krellner, and L. Taillefer, *Planar parallel phonon Hall effect and local symmetry breaking*, arXiv:2310.19682.

[40] X. Jin, X. Zhang, W. Wan, H. Wang, Y. Jiao, and S. Li, *Discovery of universal phonon thermal Hall effect in crystals*, arXiv:2404.02863.

[41] X. Li, X. Guo, Z. Zhu, and K. Behnia, *Angle-dependent planar thermal Hall effect by quasi-ballistic phonons in black phosphorus*, arXiv:2406.18816.